Supplementary Materials for

Multi-omics characterization of disulfidptosis-related molecular features to promote disulfidptosis-targeted therapy

Deze Zhao [1-6*], Yu Meng[1-5*], Yating Dian[1-5], Qian Zhou[1-5], Yuming Sun[7], Jiayuan Le[1-5], Furong Zeng[8, #], Xiang Chen[1-5#], Yi He[1-5#], Guangtong Deng[1-5#]

[*]Equal Contribution

[#]Correspondence: Guangtong Deng, dengguagntong@outlook.com;

This file includes:

Figures. S1 to S10

Supplementary Tables titles

Cell identification certificate

Supplementary Figures

Figure S1

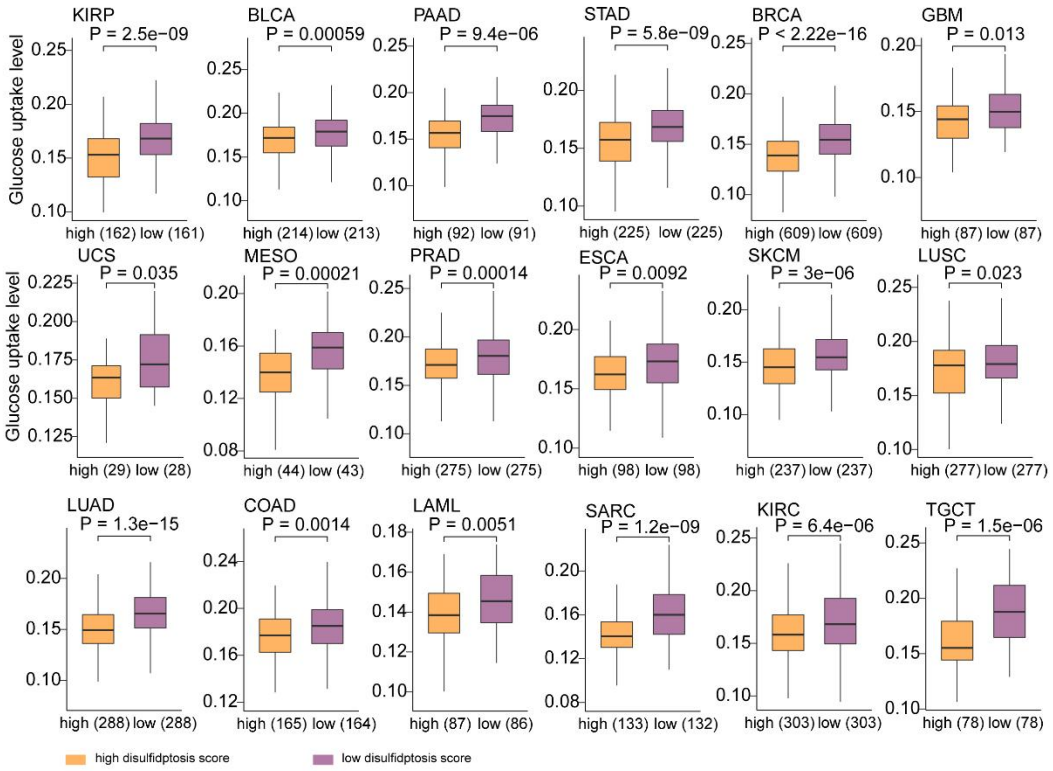

Supplementary Fig.1. Boxplot shows the difference of glucose uptake level between the Disulfidptosis score-high and Disulfidptosis score-low groups among cancer types.

Figure S2

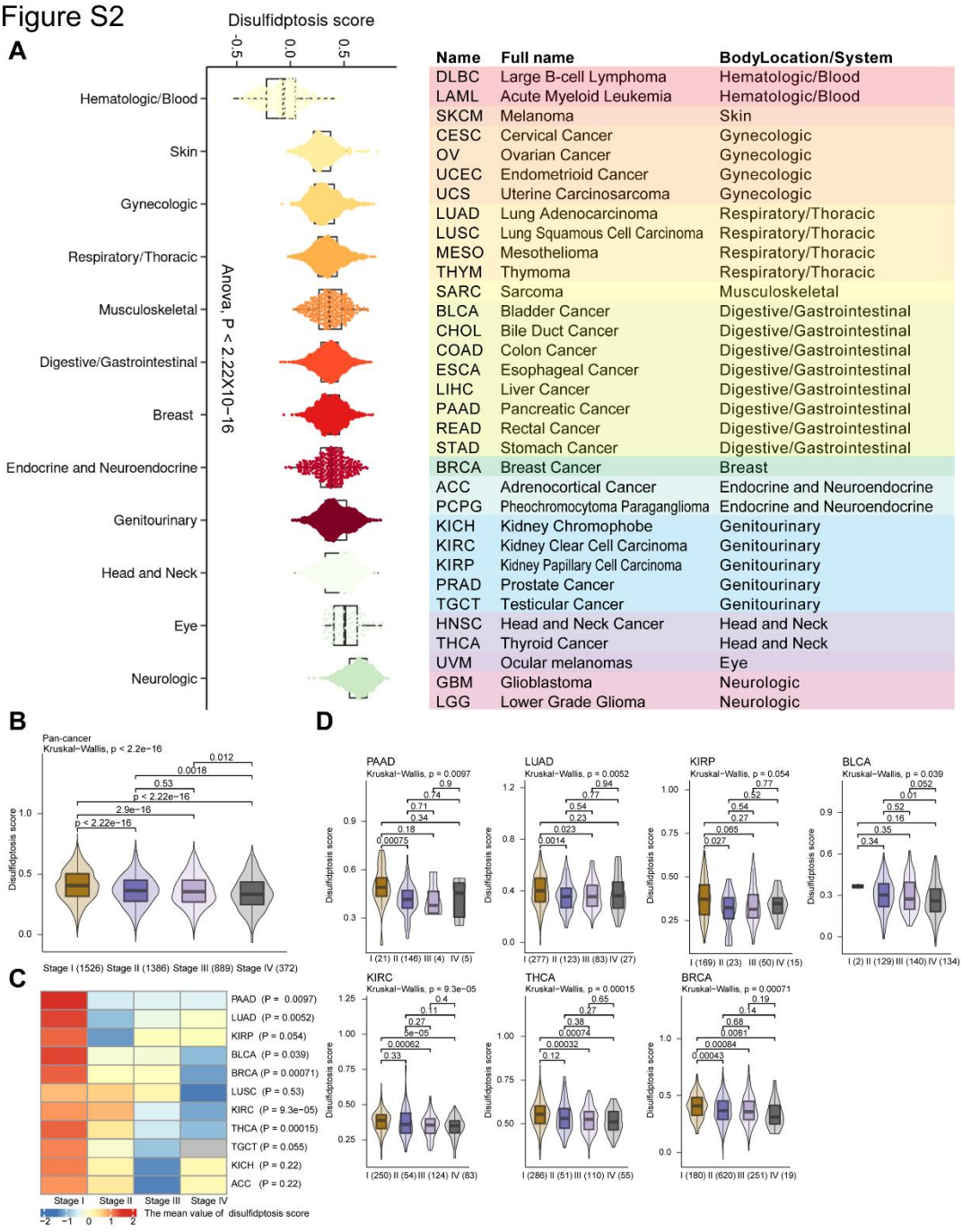

Name	Full name	BodyLocation/System
DLBC	Large B-cell Lymphoma	Hematologic/Blood
LAML	Acute Myeloid Leukemia	Hematologic/Blood
SKCM	Melanoma	Skin
CESC	Cervical Cancer	Gynecologic
OV	Ovarian Cancer	Gynecologic
UCEC	Endometrioid Cancer	Gynecologic
UCS	Uterine Carcinosarcoma	Gynecologic
LUAD	Lung Adenocarcinoma	Respiratory/Thoracic
LUSC	Lung Squamous Cell Carcinoma	Respiratory/Thoracic
MESO	Mesothelioma	Respiratory/Thoracic
THYM	Thymoma	Respiratory/Thoracic
SARC	Sarcoma	Musculoskeletal
BLCA	Bladder Cancer	Digestive/Gastrointestinal
CHOL	Bile Duct Cancer	Digestive/Gastrointestinal
COAD	Colon Cancer	Digestive/Gastrointestinal
ESCA	Esophageal Cancer	Digestive/Gastrointestinal
LIHC	Liver Cancer	Digestive/Gastrointestinal
PAAD	Pancreatic Cancer	Digestive/Gastrointestinal
READ	Rectal Cancer	Digestive/Gastrointestinal
STAD	Stomach Cancer	Digestive/Gastrointestinal
BRCA	Breast Cancer	Breast
ACC	Adrenocortical Cancer	Endocrine and Neuroendocrine
PCPG	Pheochromocytoma Paraganglioma	Endocrine and Neuroendocrine
KICH	Kidney Chromophobe	Genitourinary
KIRC	Kidney Clear Cell Carcinoma	Genitourinary
KIRP	Kidney Papillary Cell Carcinoma	Genitourinary
PRAD	Prostate Cancer	Genitourinary
TGCT	Testicular Cancer	Genitourinary
HNSC	Head and Neck Cancer	Head and Neck
THCA	Thyroid Cancer	Head and Neck
UVM	Ocular melanomas	Eye
GBM	Glioblastoma	Neurologic
LGG	Lower Grade Glioma	Neurologic

Supplementary Fig.2. (A) Disulfidptosis scores for body location of cancer types, based on the 23 disulfidptosis-related genes mRNA abundance. Body locations are sorted by the median disulfidptosis score for each body location. The right panel shows the cancers by body location/system. (B) The difference of disulfidptosis score among tumor staging. P-value was determined by Wilcoxon rank-sum test. (C) Disulfidptosis score in tumor staging of different cancer types. The color means the scaled disulfidptosis score among tumor staging. (D) The difference of disulfidptosis score among tumor staging in cancer types. P-value was accessed by Kruskal-Wallis test, followed by Wilcoxon rank-sum test.

Figure S3

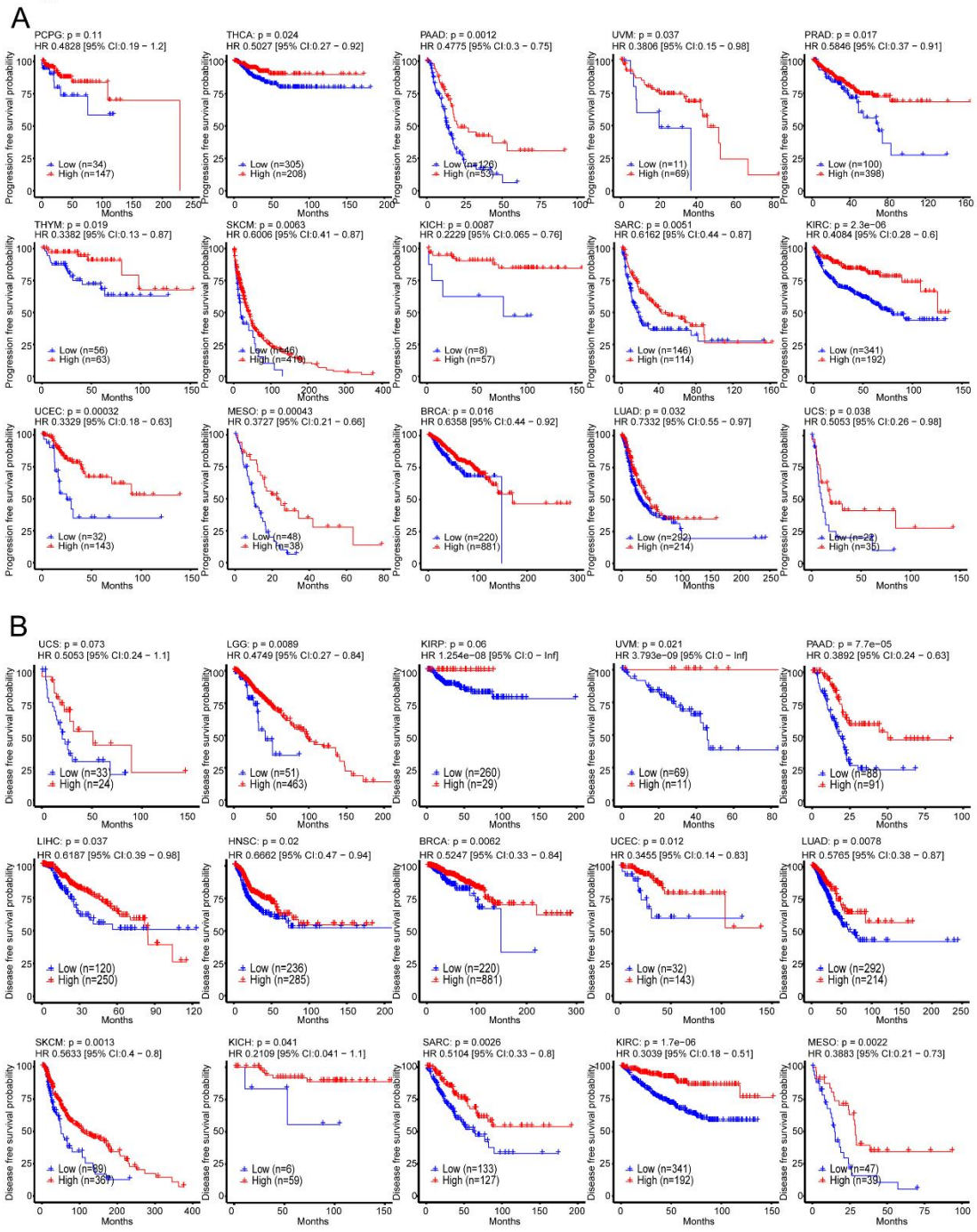

Supplementary Fig.3. The clinical relevance of disulfidptosis across cancer types. Kaplan-Meier curves show that patients with higher disulfidptosis score (red) exhibited better progression free survival times (A) and disease free survival times (B) compared to patients with lower disulfidptosis score across cancer types.

Figure S4

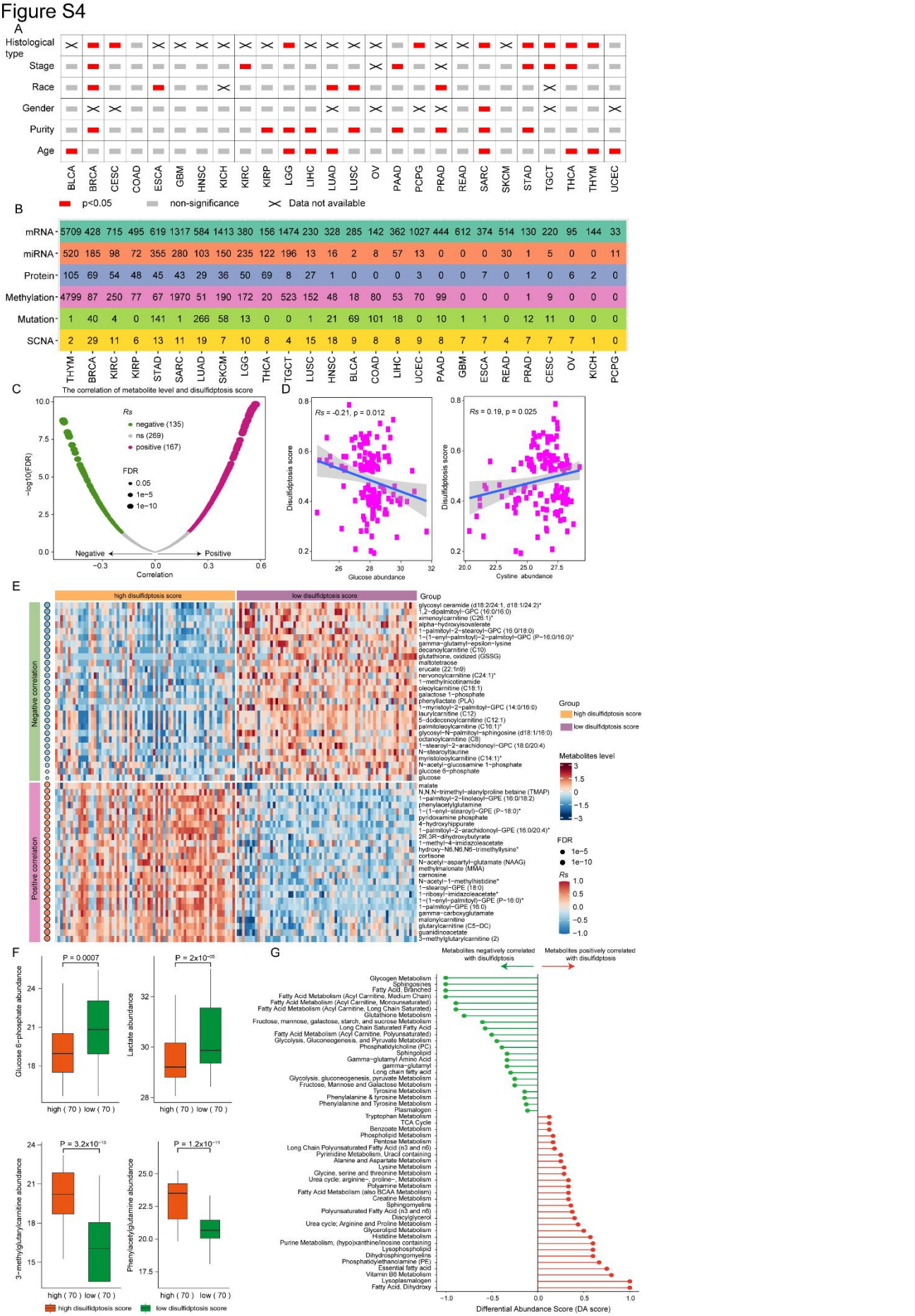
A
Histological type
Stage
Race
Gender
Purity
Age
BLCA BRCA CESC COAD ESCA GBM HNSC KICH KIRC KIRP LGG LIHC LUAD LUSC OV PAAD PCPG PRAD READ SARC SKCM STAD TGCT THCA THYM UCEC
p<0.05
non-significance
Data not available
B
mRNA 5709 428 715 495 619 1317 584 1413 380 156 1474 230 328 285 142 362 1027 444 612 374 514 130 220 95 144 33
miRNA 520 185 98 72 355 280 103 150 235 122 196 13 16 2 8 57 13 0 0 0 30 1 5 0 0 11
Protein 105 69 54 48 45 43 29 36 50 69 8 27 1 0 0 0 3 0 0 7 0 1 0 6 2 0
Methylation 4799 87 250 77 67 1970 51 190 172 20 523 152 48 18 80 53 70 99 0 0 0 1 9 0 0 0
Mutation 1 40 4 0 141 1 266 58 13 0 0 1 21 69 101 18 0 10 1 1 0 12 11 0 0 0
SCNA 2 29 11 6 13 11 19 7 10 8 4 15 18 9 8 8 9 8 7 7 4 7 7 7 1 0
THYM BRCA KIRC KIRP STAD SARC LUAD SKCM LGG THCA TGCT LUSC HNSC BLCA COAD LIHC UCEC PAAD GBM ESCA READ PRAD CESC OV KICH PCPG
C
The correlation of metabolite level and disulfidptosis score
Rs
negative (135)
ns (269)
positive (167)
FDR
0.05
1e−5
1e−10
−log10(FDR)
Negative
Positive
Correlation
D
Rs = -0.21, p = 0.012
Disulfidptosis score
Glucose abundance
Rs = 0.19, p = 0.025
Cystine abundance
E
high disulfidptosis score
low disulfidptosis score
Group
Negative correlation
Positive correlation
glycosyl ceramide (d18:2/24:1, d18:1/24:2)*
1,2−dipalmitoyl−GPC (16:0/16:0)
ximenoylcarnitine (C26:1)*
alpha−hydroxyisovalerate
1−palmitoyl−2−stearoyl−GPC (16:0/18:0)
1−(1−enyl−palmitoyl)−2−palmitoyl−GPC (P−16:0/16:0)*
gamma−glutamyl−epsilon−lysine
decanoylcarnitine (C10)
glutathione, oxidized (GSSG)
maltotetraose
erucate (22:1n9)
nervonoylcarnitine (C24:1)*
1−methylnicotinamide
oleoylcarnitine (C18:1)
galactose 1−phosphate
phenyllactate (PLA)
1−myristoyl−2−palmitoyl−GPC (14:0/16:0)
laurylcarnitine (C12)
5−dodecenoylcarnitine (C12:1)
palmitoleoylcarnitine (C16:1)*
glycosyl−N−palmitoyl−sphingosine (d18:1/16:0)
octanoylcarnitine (C8)
1−stearoyl−2−arachidonoyl−GPC (18:0/20:4)
N−stearoyltaurine
myristoleoylcarnitine (C14:1)*
N−acetyl−glucosamine 1−phosphate
glucose 6−phosphate
glucose
malate
N,N,N−trimethyl−alanylproline betaine (TMAP)
1−palmitoyl−2−linoleoyl−GPE (16:0/18:2)
phenylacetylglutamine
1−(1−enyl−stearoyl)−GPE (P−18:0)*
pyridoxamine phosphate
4−hydroxyhippurate
1−palmitoyl−2−arachidonoyl−GPE (16:0/20:4)*
2R,3R−dihydroxybutyrate
1−methyl−4−imidazoleacetate
hydroxy−N6,N6,N6−trimethyllysine*
cortisone
N−acetyl−aspartyl−glutamate (NAAG)
methylmalonate (MMA)
carnosine
N−acetyl−1−methylhistidine*
1−stearoyl−GPE (18:0)
1−ribosyl−imidazoleacetate*
1−(1−enyl−palmitoyl)−GPE (P−16:0)*
1−palmitoyl−GPE (16:0)
gamma−carboxyglutamate
malonylcarnitine
glutarylcarnitine (C5−DC)
guanidinoacetate
3−methylglutarylcarnitine (2)
Group
high disulfidptosis score
low disulfidptosis score
Metabolites level
FDR
Rs
F
P = 0.0007
Glucose 6−phosphate abundance
high (70) low (70)
P = 2x10−05
Lactate abundance
P = 3.2x10−13
3−methylglutarylcarnitine abundance
P = 1.2x10−11
Phenylacetylglutamine abundance
high disulfidptosis score
low disulfidptosis score
G
Metabolites negatively correlated with disulfidptosis
Metabolites positively correlated with disulfidptosis
Glycogen Metabolism
Sphingosines
Fatty Acid, Branched
Fatty Acid Metabolism (Acyl Carnitine, Medium Chain)
Fatty Acid Metabolism (Acyl Carnitine, Monounsaturated)
Fatty Acid Metabolism (Acyl Carnitine, Long Chain Saturated)
Glutathione Metabolism
Fructose, mannose, galactose, starch, and sucrose Metabolism
Long Chain Saturated Fatty Acid
Fatty Acid Metabolism (Acyl Carnitine, Polyunsaturated)
Glycolysis, Gluconeogenesis, and Pyruvate Metabolism
Phosphatidylcholine (PC)
Sphingolipid
Gamma−glutamyl Amino Acid
gamma−glutamyl
Long chain fatty acid
Glycolysis, gluconeogenesis, pyruvate Metabolism
Fructose, Mannose and Galactose Metabolism
Tyrosine Metabolism
Phenylalanine & tyrosine Metabolism
Phenylalanine and Tyrosine Metabolism
Plasmalogen
Tryptophan Metabolism
TCA Cycle
Benzoate Metabolism
Phospholipid Metabolism
Pentose Metabolism
Long Chain Polyunsaturated Fatty Acid (n3 and n6)
Pyrimidine Metabolism, Uracil containing
Alanine and Aspartate Metabolism
Lysine Metabolism
Glycine, serine and threonine Metabolism
Urea cycle; arginine−, proline−, Metabolism
Polyamine Metabolism
Fatty Acid Metabolism (also BCAA Metabolism)
Creatine Metabolism
Sphingomyelins
Polyunsaturated Fatty Acid (n3 and n6)
Diacylglycerol
Urea cycle; Arginine and Proline Metabolism
Glycerolipid Metabolism
Histidine Metabolism
Purine Metabolism, (hypo)xanthine/inosine containing
Lysophospholipid
Dihydrosphingomyelins
Phosphatidylethanolamine (PE)
Essential fatty acid
Vitamin B6 Metabolism
Lysoplasmalogen
Fatty Acid, Dihydroxy
Differential Abundance Score (DA score)

Supplementary Fig.4. Propensity score algorithm and the disulfidptosis-related molecular patterns altered in cancer types. (A) Potential confounding factors between disulfidptosis score-high and disulfidptosis score-low tumors across 26 cancer types. Heatmap shows p-values (two-sided t-test for continuous variables, including age at diagnosis and tumor purity, and chi-squared test for discrete variables, including gender, race, pathologic stage, and histological type) with significance ($p < 0.05$, red). Features marked as X indicate data not available. (B) Heatmap shows the number of each altered molecular features (mRNA, miRNA, methylation, mutation, protein, and SCNA) in disulfidptosis score-high (red) and disulfidptosis score-low (blue) groups from TCGA tumor samples. (C) Pearson's correlation between metabolite level and disulfidptosis score. Magenta point: $Rs > 0.18$, $FDR < 0.05$; green point: $Rs < -0.18$, $FDR < 0.05$; gray point: non-significant correlation (ns). (D) Scatter plot at the left panel shows the significant negative correlation between glucose abundance level and disulfidptosis score, and the right panel shows the significant positive correlation between cystine abundance level and disulfidptosis score (pearson's correlation). (E) Heatmap shows the significant alteration between disulfidptosis score-high samples ($n = 70$) and disulfidptosis score-low samples ($n = 70$) in ccRCC. The left panel shows the metabolites most significantly associated with the disulfidptosis score. (F) Boxplot shows the difference of metabolites level (such as Glucose 6-phosphate, lactate, 3-methylglutarylcarnitine and phenylacetylglutamine) between the Disulfidptosis score-high and Disulfidptosis score-low groups. (G) Pathway-based analysis of metabolic changes in metabolites positively correlated (yellow dot) vs. negatively (blue dot) correlated with disulfidptosis score. The differential abundance (DA) score > 0 indicates pathways enriched for metabolites that are positively correlated with disulfidptosis ($n=167$), and the DA score < 0 indicates pathways enriched for metabolites that are negatively correlated with disulfidptosis ($n=135$).

Figure S5

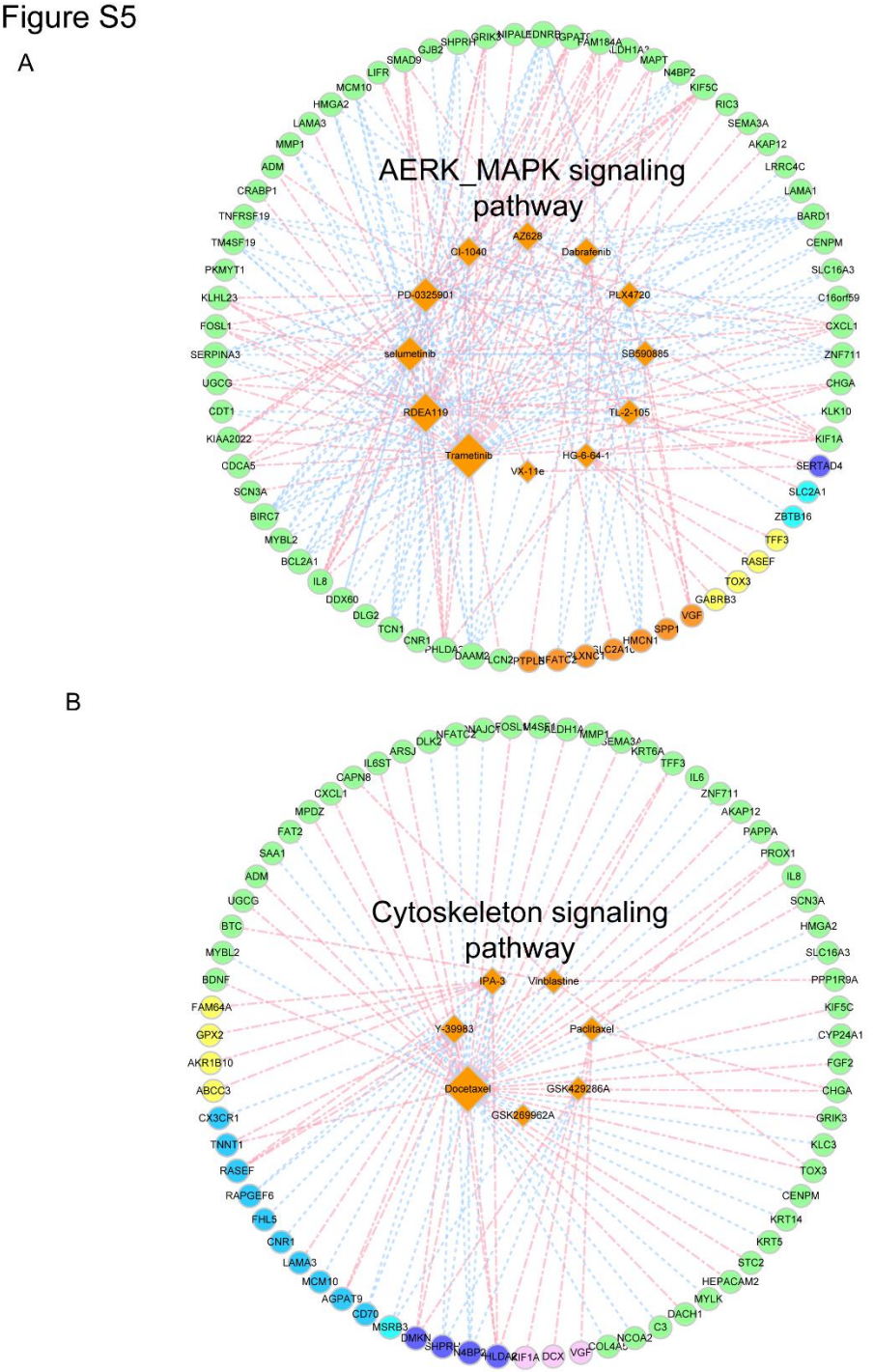

Supplementary Fig.5. Disulfidptosis-related genes (green point) correlate to drug-sensitive (cyan) or drug-resistant (magenta) response to drug (orange point) involved in signaling pathways. (A) ERK/MAPK signaling pathway, (B) cytoskeleton signaling pathway.

Figure S6

Supplementary Fig 6. Disulfidptosis-related miRNA and protein signatures. (A) Altered miRNA in the disulfidptosis score-high group vs. the disulfidptosis score-low group for multiple cancers. Color indicates the difference in miRNA expression; point size indicates FDR for miRNA expression. (B) Barplot shows the Significant Kyoto Encyclopedia of Genes and Genomes (KEGG) pathways enriched by mRNAs in the miRNA-target regulatory network. (C) The Spearman's correlation between disulfidptosis score and the infiltration level of 22 immune cell types in pan-cancers (n = 10 205). Black box indicates the significant correlations (|Rs| > 0.2 and FDR < 0.05). (D) Spearman's correlation between protein level of YAP (ps127) and imputed

drug response in five cancer types. The green point denotes drug sensitivity; the magenta point denotes drug resistance.

Figure S7

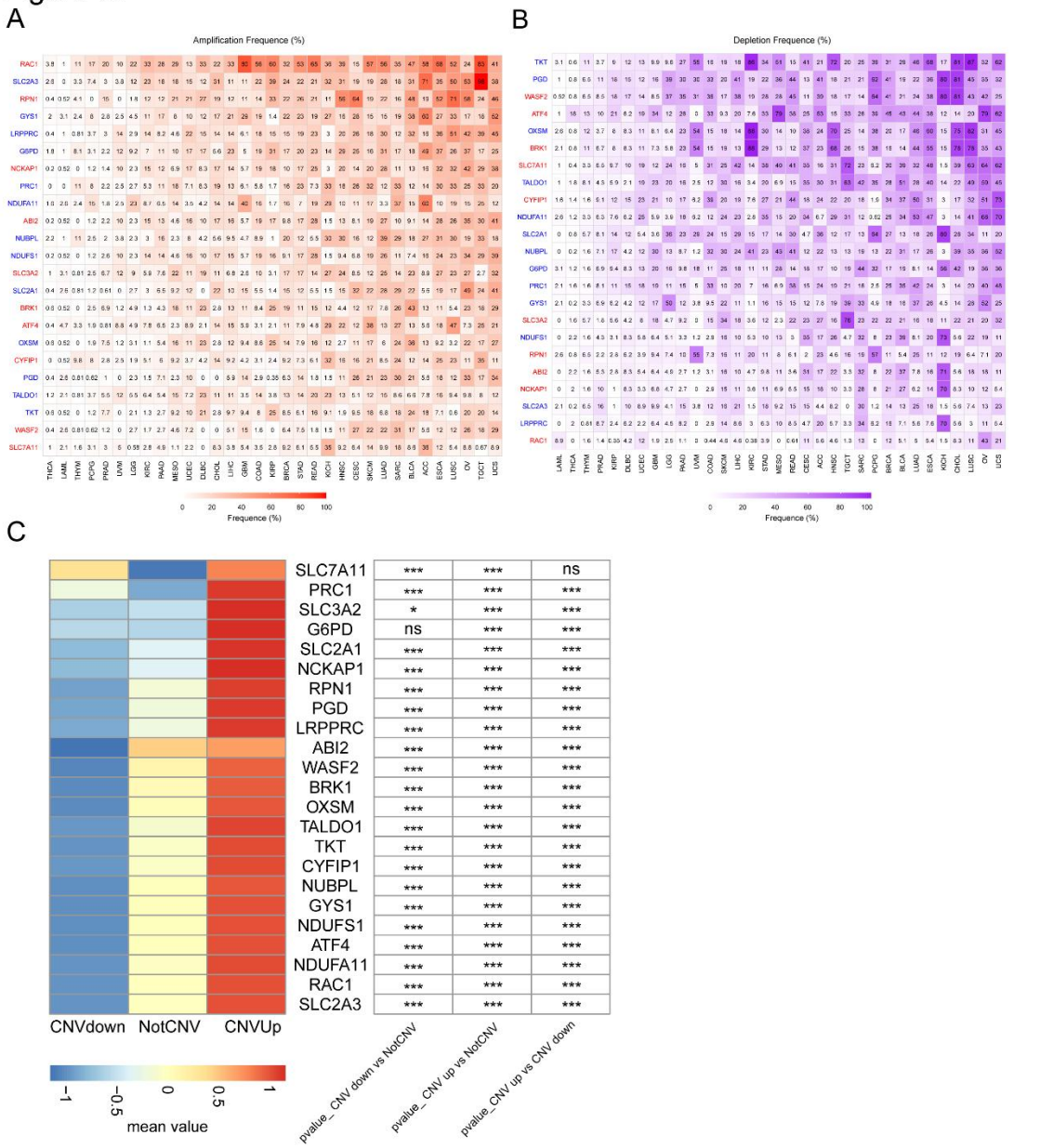

Supplementary Fig 7. Somatic copy number alterations of disulfidptosis regulators in cancer. (A-B) Distribution of amplification (A), and deletion (B) frequencies of 23 disulfidptosis signatures over cancer types. The numbers in the graph represent the specific frequency values. The intensity of color is proportional to the frequency. (C) The expression of 23 disulfidptosis signatures among somatic copy number alterations groups in TCGA tumor samples from 26 cancer types.

Figure S8

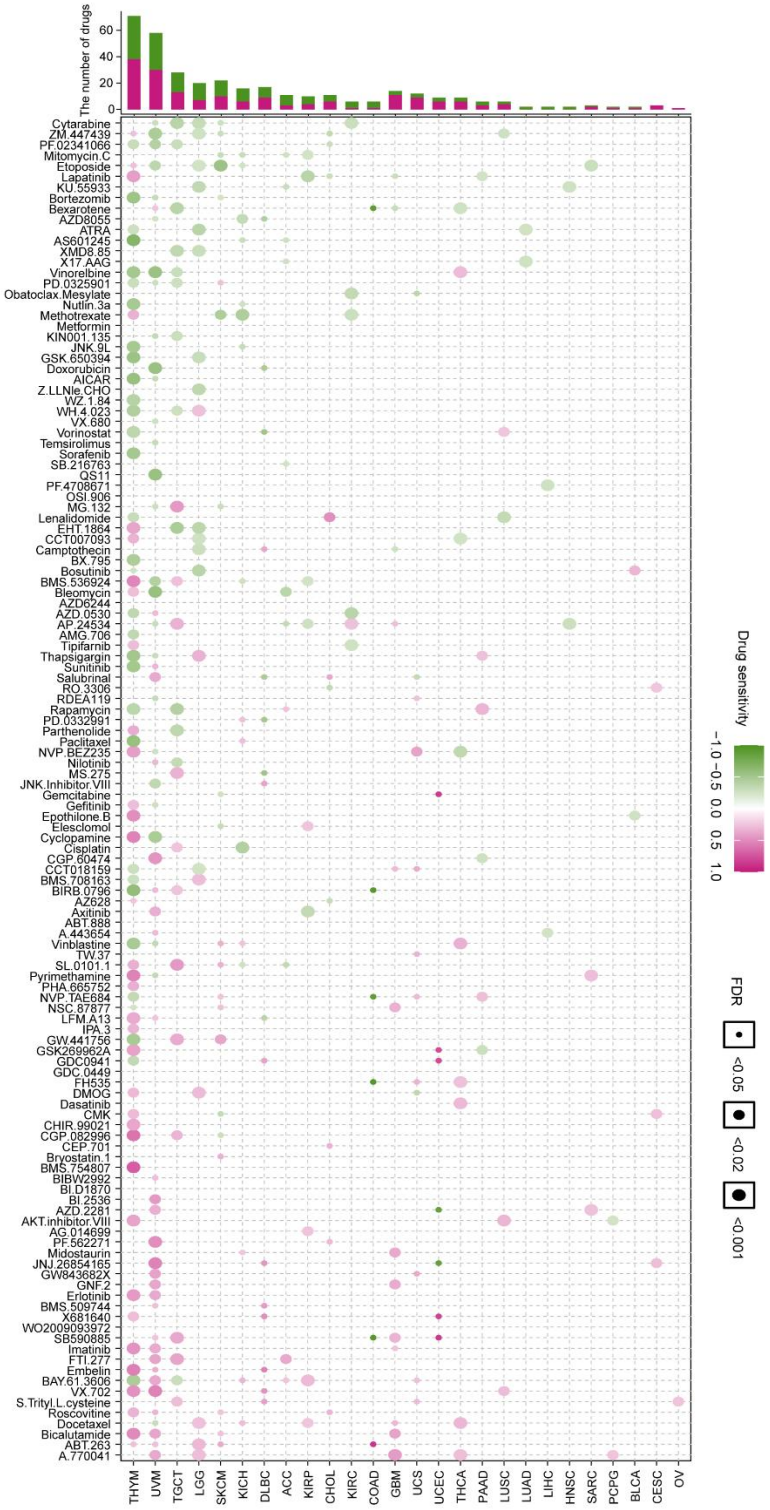

Supplementary Fig.8. The disulfidptosis effects on drug response. Spearman's correlation between imputed drug response and disulfidptosis score across 26 cancer types in TCGA patients. The bar plot (top panel) shows the number of drugs that positively (magenta, drug-resistant) and negatively (green, drug-sensitive) correlate to the disulfidptosis score in each cancer type.

Figure S9

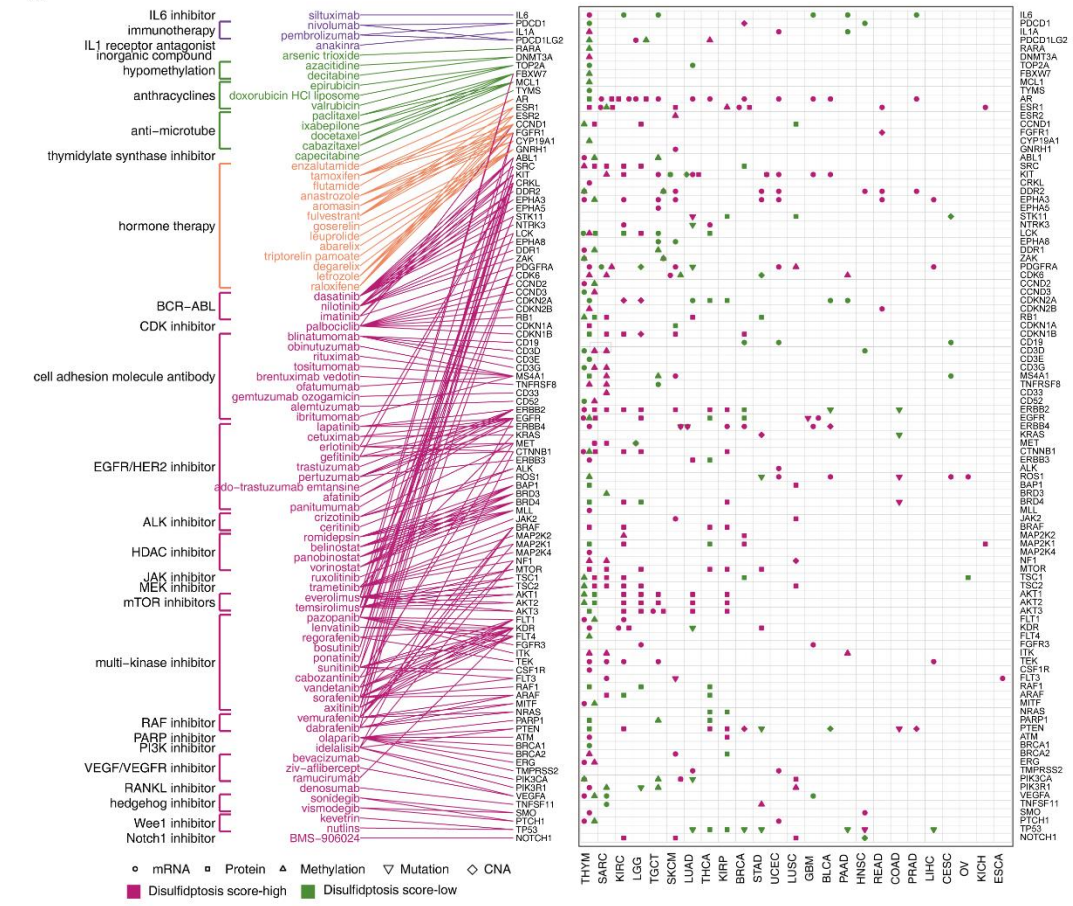

Supplementary Fig 9. Summary characteristics of FDA-approved drugs and their linked clinically actionable genes (left) and alterations of these genes at mRNA, protein, DNA methylation, mutation and SCNA levels based on disulfidptosis score-high (magenta) or score-low (green) samples across 26 cancer types (right). The different symbol shapes represent different types of molecular data.

Figure S10

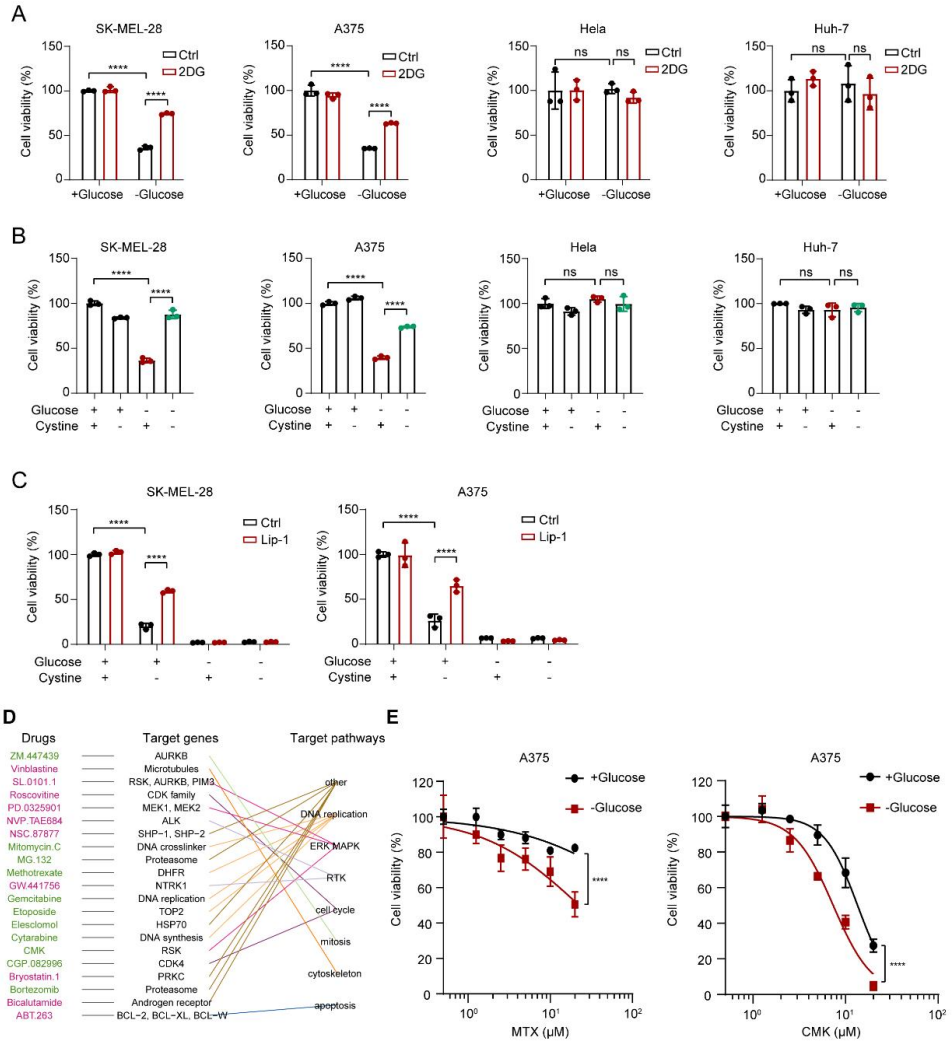

Supplementary Fig 10. (A) Relative cell viability in the SK-MEL-28, A375 (Red label; Disulfidptosis-score high), HeLa and Huh-7 (Green label; Disulfidptosis-score low) cells cultured in glucose-containing (+Glucose) or glucose-free (-Glucose) medium with or without 2 mM 2-Deoxy-D-glucose (2DG) for about 16 hours. (B) Relative cell viability in the SK-MEL-28, A375 (Red label; Disulfidptosis-score high), HeLa and Huh-7 (Green label; Disulfidptosis-score low) cells cultured in glucose-containing, cystine-free, glucose-free, or glucose/cystine double-free medium for about 16 hours. (C) Relative cell viability in the SK-MEL-28 and A375 cells cultured in glucose-containing, cystine-free, glucose-free, or glucose/cystine double-free medium with or without 10 μM liproxstatin-1 (lip-1) for about 36 hours. (D) The targeted genes and targeted pathways of drugs in disulfidptosis status in TCGA-SKCM. (E) Dose-response curves for relative cell viability of methotrexate and CMK in glucose-containing (+Glucose) and glucose-free (-Glucose) conditions in the A375 melanoma cells.

Supplementary Tables

Supplementary Table 1. Summary of disulfidptosis-related features. A total of 23 disulfidptosis-related genes were collected from published articles.

Supplementary Table 2. Disulfidptosis scores for 25 types of cancer that including 760 cancer cell lines.

Supplementary Table 3. Spearman's rank correlation between disulfidptosis-related mRNA expression levels and drug sensitivity (AUC value) across pan-cancer.

Supplementary Table S4： Spearman's rank correlation between disulfidptosis-related proteins expression levels and drug sensitivity (AUC value) across pan-cancer.

Supplementary Table S5： Spearman＇s rank correlation between disulfidptosis-related miRNAs expression levels and drug sensitivity (AUC value) across pan-cancer.